Lattice dynamics of tetrahedrally bonded semiconductors containing ordered vacant sites*

E. Finkman† and J. Tauc
Division of Engineering and Department of Physics, Brown University, Providence, Rhode Island 02912

R. Kershaw and A. Wold
Division of Engineering and Department of Chemistry, Brown University, Providence, Rhode Island 02912

(Received 16 December 1974)

Infrared and Raman spectra of defect-structure semiconductors In_2Te_3, Ga_2Se_3, and Ga_2S_3 with ordered vacant sites were measured on polycrystalline samples and analyzed. The interpretation of the observed spectra is based on the existence of uninterrupted chains of tetrahedra along the directions interconnecting the two next-nearest neighbors (the [110] direction in the cubic lattice). Arguments are presented to show that the phonons propagating along this direction dominate the spectra, and that in the first approximation their frequencies can be obtained by a sixfold folding of the Brillouin zone of the simple zinc-blende structure in the [110] direction. The observed spectra were fitted by a rigid-ion model of the corresponding zinc-blende structure, and the dispersion relations for this structure were obtained. It is shown that the defects affect the central forces between the nearest neighbors only slightly while the noncentral forces are changed more significantly. The softening of a mode in In_2Te_3 may point out an instability of its ordered structure.

I. INTRODUCTION

M_2X_3 compounds (where M = Al, Ga, or In and X = S, Se, or Te) are the simplest examples of materials whose structure is based on the tetrahedral atomic coordination as in the zinc-blende (ZB) structure, but in which some atomic sites are empty.[1,2] In the case of M_2X_3 compounds one-third of the cation sites of the ZB or wurtzite structures available to group-III atoms is vacant. It is apparent from the chemical formula that the valencies are satisfied. In some of these compounds the vacancies can be ordered and form a superlattice below a certain temperature. A number of authors have studied the structural,[3–10] electrical,[11,12] and optical properties[13–20] of some M_2X_3 compounds. We report here the infrared and Raman studies of lattice vibrations in In_2Te_3, Ga_2Se_3, and Ga_2S_3. Since the unit cell of these compounds with ordered vacancies contains a very large number of atoms we would expect that the infrared and Raman spectra contain many lines. We observed,[21] however, a relatively small number of Raman and infrared lines which appear to be related in a simple way to the vibrational spectra of the perfect ZB structure. We present our experimental data, and then discuss how they can be understood on the basis of the spatial arrangement of defects in the ZB structure. We believe that the basic ideas of this approach may prove useful more generally, in particular for the analysis of vibrations in a complicated crystal structure, which is composed of some simple structural elements.

II. MATERIALS PREPARATION

A. In_2Te_3

Stoichiometric quantities of high-purity indium and tellurium (99.999%) were reacted in evacuated, sealed silica tubes. The reaction was performed in a specially constructed furnace, which rocked the samples back and forth through a 15° arc 10 times per minute. This was done to avoid segregation of the molten mixture, and promote rapid, complete reaction of the charge.

The temperature of the furnace was raised to 800 °C over a 3-h period, and the charge of indium and tellurium was reacted for 3 days. The rocking motion was then stopped, the furnace was turned to the vertical position so that all of the melt would be at the bottom of the sealed silica tube, and the furnace was shut off. The sample was allowed to cool in the furnace overnight. This produced a polycrystalline ingot of In_2Te_3 with ordered vacancies ("ordered" In_2Te_3). X-ray powder diffraction showed it to be cubic, with $a_0 = 18.48$ Å.

In_2Te_3 was also prepared in the disordered phase, where $a_0 = 6.16$ Å. This was accomplished by heating a sample of the ordered phase, prepared as described, to 725 °C. The sample was held at this temperature for 8 hs, and was then cooled to 670 °C at the rate of 10 °C/h. It was held at 670 °C for 24 h and then quenched into ice water.

B. Ga_2Se_3

Ga_2Se_3 was prepared by reacting stoichiometric quantities of gallium and selenium in the previously described rocking furnace. The sample was initially heated to 600 °C; the furnace temperature

was then raised in 100 °C increments every 4 h to a final temperature of 1050 °C. After 8 h at this temperature the furnace was turned off and the sample allowed to cool overnight. This resulted in the formation of a polycrystalline ingot.

To obtain a greater degree of crystallinity, and to form the ordered phase,[10] samples with the stoichiometry corresponding to $Ga_2Se_{3.04}$ were prepared as above and were then loaded into a Bridgman-type silica crucible. They were melted at 1050 °C, and then lowered through a 20 °C/cm temperature gradient at the rate of 1 cm/day down to 950 °C. The sample was then placed in a furnace at 600 °C for 1 week. This treatment was used to produce a much better crystalline sample with ordered structure. Identical experiments in which the stoichiometry of the reactants was Ga_2Se_3 did not produce the ordered phase.[10]

C. Ga_2S_3

Ga_2S_3 was prepared by reacting high-purity gallium with H_2S. A silica boat, containing the gallium, was heated in an atmosphere of flowing H_2S at 900 °C for 4 h. The multiphase product thus obtained was ground with an agate mortar and pestle for 1 h in a dry box under a dry nitrogen atmosphere. Two additional 4-h firings in H_2S at 950 °C with an intermediate grinding, produced the ordered phase Ga_2S_3. A disordered phase was not observed to form.

III. EXPERIMENTAL RESULTS

Far-infrared spectra were measured at room temperature with an evacuated Digilab model FTS-14 Fourier spectrometer. A condensing specular-reflectance accessory made by Harrick was used for the reflectivity measurements. We redesigned the sample holder so that the sample could be placed with its face down on a horizontal platform with an appropriate aperture. This arrangement allowed us to have the sample and the reference mirror exactly at the same place.

Raman spectra were measured in the backscattering configuration. For Ga_2Se_3 we used the 6200-Å line from a Coherent Radiation model 450 dye laser which was pumped with a Coherent Radiation model 52B argon-ion laser. Raman spectra of In_2Te_3 were measured using the 5145-Å line of the model 52B laser. The spectra were analyzed with a Jarrel-Ash 22-150 double-grating monochromator with an additional third $\frac{1}{4}$-m Jarrel-Ash monochromator placed in front of the photomultiplier to further reduce the stray laser light. We measured the depolarization ratio of the Raman scattering in our polycrystalline materials. All the lines were found to be depolarized, and these measurements were not useful for the line assignment.

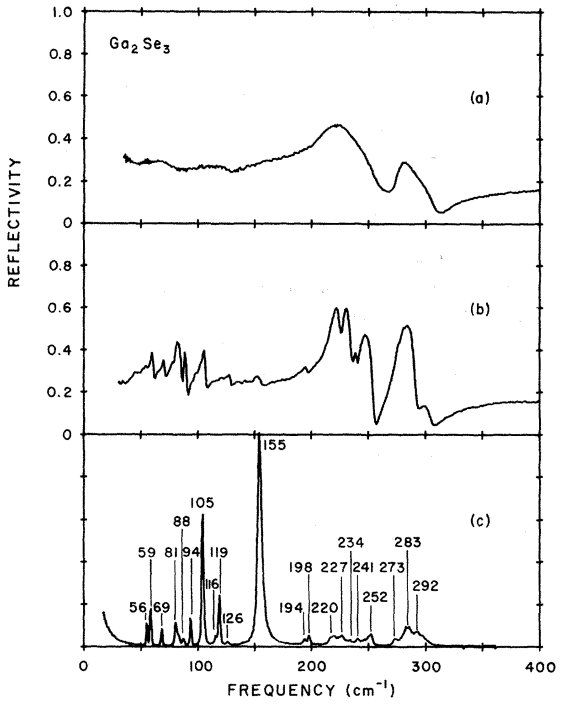

FIG. 1. Infrared reflectivity for disordered (a) and ordered (b) Ga_2Se_3. Curve (c) shows the unpolarized Raman spectrum for ordered Ga_2Se_3.

The infrared and Raman spectra of polycrystalline Ga_2Se_3 at room temperature are given in Fig. 1. We used the Kramers-Kronig analysis of the infrared reflection data of ordered Ga_2Se_3 and the results in terms of the imaginary parts of ϵ and $-1/\epsilon$ are shown in Fig. 2. The peaks give the transverse and longitudinal frequencies of the infrared active modes, respectively. The Raman spectrum shows almost identical modes to the infrared spectrum. Some of the lines which appear as singlets in the infrared spectrum (e.g., those at 60, 71, 84, and 196 cm^{-1}) resolve into doublets in the Raman spectrum. Their splitting is too large (3 to 4 cm^{-1}) to be accounted for by the LO-TO splitting (which is about 1 cm^{-1} as seen in Fig. 2). One Raman doublet at 116 and 119 cm^{-1} does not show up in the infrared reflection and might be absorbed in the noise.

The Raman spectra of polycrystalline In_2Te_3 at room temperature (Fig. 3) are dominated by lines characteristic of crystalline tellurium which are the same in the ordered or disordered material. An interesting feature of these tellurium Raman lines is that the low E_{LO} mode at 105 cm^{-1} is a dominant line in our spectrum while it is hardly observable in pure tellurium.[22] Some weak additional lines observed in ordered In_2Te_3 correspond to those of the infrared spectrum[21] (Fig. 3). The results of an oscillator fit to the reflectivity of

In_2Te_3 are shown in Fig. 4.

Only infrared absorption data were taken for Ga_2S_3. The result obtained on a powdered sample at room temperature is shown in Fig. 5. Raman measurements for our powdered sample were unsuccessful because of a very intense fluorescence.

IV. STRUCTURE

As mentioned above, the structures of many M_2X_3 compounds are based on the sphalerite and wurtzite structures which have tetrahedral bonding. In these cases every group-III atom is surrounded by four group-VI atoms. One-third of the tetrahedral sites around the group-VI atoms are vacant on the average. All aluminum and gallium chalcogenides of the M_2X_3 type crystallize in tetrahedral structures. Among the indium compounds only In_2Te_3 belongs to the above group. First studies of these materials showed random distribution of the vacancies.[3] Later, it was found that in some of the M_2X_3 compounds the vacant sites can be ordered. The reported structures[3–10] have all been based on a close packing of the group-VI atoms with the following assumptions generally accepted for the ordering of the group-III atoms: (i) Only tetrahedral sites are occupied. (ii) No group-VI atom with less less than two nearest group-III-atom neighbors is allowed.

In this section we will first briefly discuss the structures which were reported in the literature for the ordered modifications of In_2Te_3,[5,6,8] Ga_2S_3,[9] and Ga_2Se_3,[10] and summarize some of their general features which will be used later in analyzing the infrared and Raman modes of these crystals.

The ordered structure of In_2Te_3 is somewhat controversial as three different structures are reported in the literature. We shall discard the "antifluorite" structure suggested by Holmes[5] because it does not satisfy assumption (i). Wooley

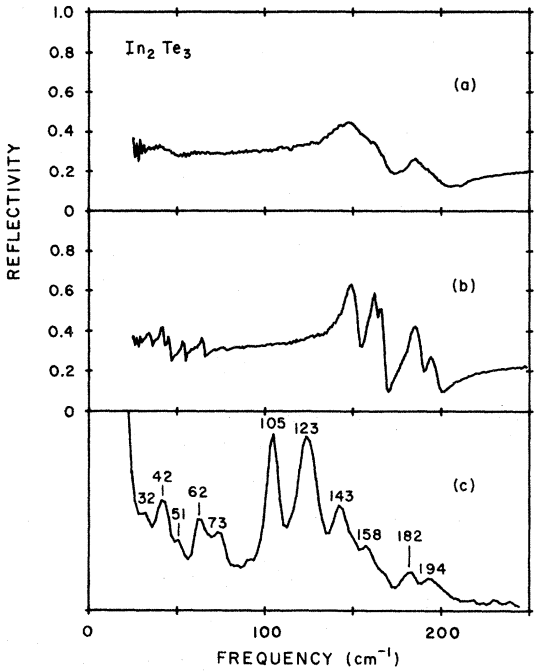

FIG. 3. Infrared reflectivity for disordered (a) and ordered (b) In_2Te_3. Curve (c) shows the unpolarized Raman spectrum of ordered In_2Te_3. The strong Raman lines at 105, 123, and 143 cm^{-1} are characteristic of crystalline Te (Ref. 22).

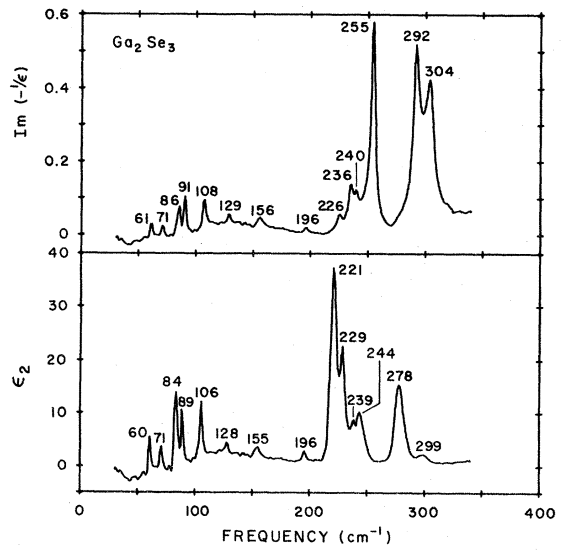

FIG. 2. Results of Kramers-Kronig analysis of the reflection infrared spectrum of Ga_2Se_3.

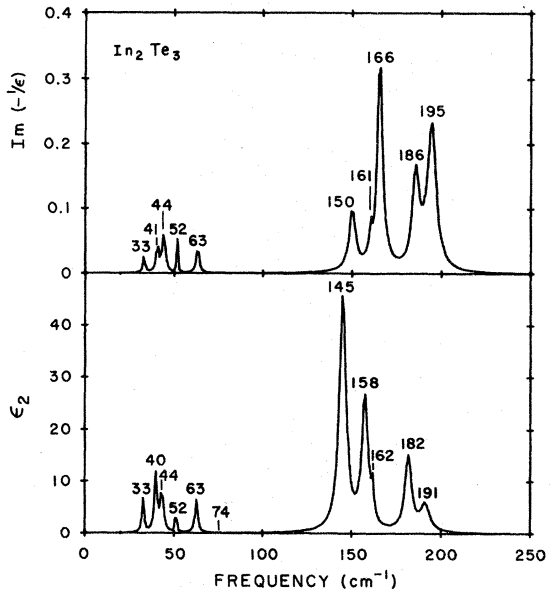

FIG. 4. Results of an oscillator fit to the reflectivity of ordered In_2Te_3. The oscillator parameters were taken from Ref. 21.

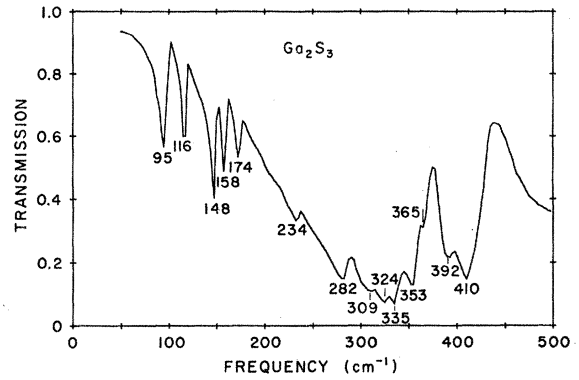

FIG. 5. Infrared absorption data for Ga_2S_3. The powdered sample was spread on a polyethylene substrate.

and Pamplin[5] suggested a body-centered orthorhombic structure (space group $Imm2$) with two formula units per unit cell. This structure is shown in Fig. 6. Although it does not seem to represent correctly the crystal structure, it is shown here because of its simplicity and because of a general structural feature it has which is common to all the structures which we will consider. This is that the group-III atoms form uninterrupted chains in a direction connecting two next nearest neighbors, which is equivalent to the [110] direction of the cubic lattice.

In the particular structure shown in Fig. 6, the vacancies and adjacent Te atoms also form continuous chains through the lattice in this direction, and every third cubic (110) layer is emptied of all its indium atoms. The unit cell contains six Te layers in the [110] cubic direction. However, there are two experimental facts which are not compatible with this particular structure. First, one would expect that such a structure would contract in the [110] direction as is the case for some M_2X_3 ordered compounds (e.g., Ga_2S_3 and Ga_2Se_3). However, no anisotropic distortion is observed for[5] In_2Te_3 within the experimental accuracy reported. Second, we might expect easy cleavage along the (110) planes. However, the observed angle between two cleavage planes in this crystal is 70.5°, which characterizes the intersection of two (111) planes. In fact, Zaslawskii *et al.*[6] have shown that the cleavage planes are perpendicular to a threefold symmetry axis. They have reported x-ray data which indicate that the structure of ordered In_2Te_3 is cubic with a space group of $F\bar{4}3m$. These observations seem to confirm earlier predictions[4,8] that In_2Te_3 has a cubic unit cell with $a = 3a_0$ and $a_0 = 6.16$ Å being the dimension of the basic ZB unit cell. The unit cell of In_2Te_3 contains 36 formula units.

Some difficulties arise, however, with Zaslawskii's proposed face-centered-cubic space group $F\bar{4}3m$. We tried to construct the fcc large unit cell but symmetry considerations forced us to include at least four Te atoms which were surrounded by a tetrahedron whose apices were vacant sites. This result was discarded and a threefold simple-cubic primitive cell was tried instead. If the unit cell is simple cubic, the x-ray diffraction pattern would show additional lines relative to the fcc unit cell. The appearance of weak diffraction peaks associated with the simple-cubic (sc) structure may be difficult to observe.

We constructed many possible sc strucutres but most of them contained complete tetrahedra of vacancies and were discarded. None of these structures was found to satisfy assumption (ii). This contradicts Wooley and Pamplin's[5] report that such a structure exists. Ten primitive cells were constructed in which no Te atom was surrounded by a complete tetrahedron of vacancies. These structures, however, contain at least four Te atoms which have three vacancies as nearest neighbors. These considerations did not allow us to make a definite decision about the actual unit cell of In_2Te_3. However, one important feature was observed in all the constructed structures. Unbroken continuous chains of In atoms extend in [110] directions throughout the lattice. This is apparent from an example of one of the possible structures shown in Fig. 7.

For Ga_2Se_3 the ordered crystal structure is based on the ZB structure but is noncubic. The unit cell is reported[19] to be orthorhombic ($a = 7.760$, $b = 11.640$, $c = 10.822$ Å) with eight formula units and the space group is D^8_{2h}. As no detailed analysis of the x-ray spectrum has been done the exact structure is unknown. We only mention that there exists a slight distortion from the ideal cubic case as a result of a contraction of about 1.5% along two orthogonal [110] directions of the cubic basis. As mentioned in Sec. II, the materials actually studied

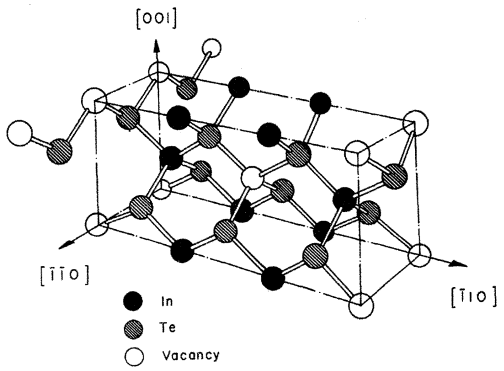

FIG. 6. Ordered structure of In_2Te_3 as suggested by Wooley and Pamplin (Ref. 5). The directions are related to the cubic zinc-blende cell.

were slightly nonstoichiometric.

For Ga_2S_3 the structure of the ordered material is based on wurtzite.[9] The distortion along the next-nearest-neighbor direction is about 9% and the space group is monoclinic $C1c1$; $a = 11.14$, $b = 6.41$, $c = 7.03$ Å, $\beta = 121.22°$, and the unit cell contains four formula units.

It is found that in all the above-mentioned ordered M_2X_3 structures vacancies occur most frequently along the original cubic [110] direction (along the [100] direction in structures based on the hexagonal lattice). Uninterrupted chains of the group-III atoms extend along the same directions. The period of all the primitive cells along this direction is six tetrahedra.

The existence of continuous, unbranched chains of vacancies and group-VI atoms was first discussed by Newman.[23] We believe that the existence of uninterrupted chains of group-III atoms occurs under more general conditions than those assumed by Newman, and are common to all the ordered structures of M_2X_3 based on the tetrahedral bonding. Since the group-III atoms are surrounded by four group-VI atoms there are uninterrupted chains of tetrahedra in the directions equivalent to the [110] direction of the cubic lattice (that is in the direction interconnecting the two next nearest neighbors).

V. DISCUSSION

The most striking observation about the spectra is their simplicity. The smallest unit cell that can be constructed for an ordered M_2X_3 compound contains two formula units (e.g., the orthorhombic cell in Fig. 6). This will result in $3 \times 10 - 3 = 27$ nondegenerate optical vibrational modes at $k = 0$. The structures discussed above for In_2Te_3, Ga_2S_3, and Ga_2Se_3 contain many more atoms per unit cell and yet the spectra consist of a small number of lines most of which are very sharp.

A second important feature of the experimental results is the great similarity between the spectra of the three ordered materials despite the completely different crystal structures. All exhibit two groups of high-energy lines, and a group of low-energy lines. The frequencies of the spectral lines scale with an almost constant scaling factor between the different materials.

It is anticipated, of course, that general features of the spectra in these materials will be characterized by the short-range tetrahedral bonding which is common to all of them. The actual structure of the spectra, however, is expected to be related to the long-range crystal structure. The detailed resemblance of the infrared and Raman spectra of the three materials suggests that the similarity is related to the common long-range-order features discussed in Sec. IV.

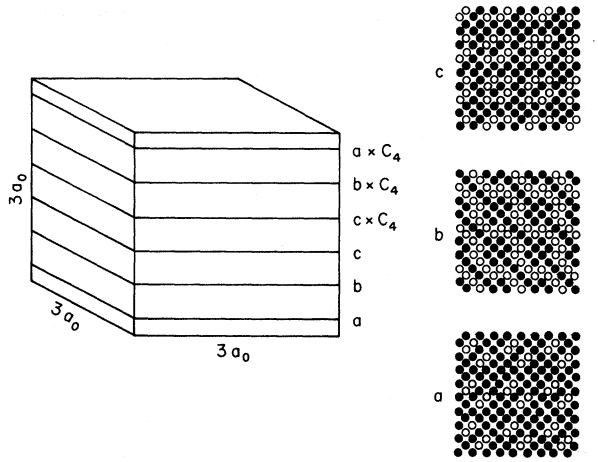

FIG. 7. Possible ordered structure for a simple cubic unit cell of In_2Te_3. Three out of the six layers of In (full circles) and vacancies (open circles) in the (100) planes are shown. The other three ($a \times C_4$, $b \times C_4$, $c \times C_4$) can be obtained from them by a rotation of 90°, denoted by C_4 in the figure. In the right-hand figures, each layer is extended to 3×3 unit cells in order to demonstrate the existence of uninterrupted chains in the [110] direction. All the available sites for the Te atoms are filled and are not shown in this figure.

An exact analysis of the optically active phonons of the actual crystal structure based on the usual methods would be complicated. We would have to determine not only the symmetries and frequencies of the phonons at $k = 0$ but deal also with the intensities to account for the small number of the actually observed lines. We believe that the approach which we discuss below provides more physical insight into the problem of vibrations in defect structures.

Our basic assumption is that, to a first approximation, the vibrational modes in the defect structures will not differ very much from those found in the ZB structures without defects.[21] In particular their frequencies are assumed to change only slightly. This assumption is in agreement with the theoretical considerations of Van Vechten and Thurmond[24] who calculated the change of the entropy of a solid by the introduction of vacancies. From the comparison of their theory with the experimental data for Ge and Si they concluded that the changes of the lattice-mode frequencies by the presence of vacancies are small. We assume that the primary effect of the vacancies is a change in the k-vector conservation selection rules.

Since the dimensions of the unit cell of the defect structures are always larger than those of the ZB unit cell, the Brillouin zone (BZ) of the defect structure (the "real" BZ) is smaller than the BZ of the ZB structure (the "large" BZ). All reciprocal-lattice points of the defect structure which are

inside or at the zone boundaries of the larger BZ are equivalent to $k=0$. Therefore, the vibrations corresponding to these k vectors in the large BZ can be optically active.

Let us consider, for example, the case of ordered In_2Te_3. If we assume a simple-cubic primitive unit cell for this structure, its lattice constant is 6 times larger than that of the primitive cell of the ZB structure.[25] Therefore, the k-space periodicity of ordered In_2Te_3 is 6 times smaller than that of the ZB structure for which the reciprocal-lattice vectors are $(4\pi/a)(n_1, n_2, n_3,)$. The reciprocal-lattice vectors in the real BZ are $(2\pi/3a)(n_1, n_2, n_3)$. All those points within the large BZ or on its surface may become optically active in addition to the original $k=0$ modes.

The above considerations enable us to apply the relatively simple solution of the dynamical matrix of the ZB structure for the calculations of the frequencies of the real structure. Nine different points in the large BZ are expected to be folded into the zone center: all the points $(2\pi/3a)(n_1, n_2, n_3)$ for which $n_i=0$, 1, 2, or 3 and $n_1+n_2+n_3\leq 4$; other folded points (allowing also negative values of n_i) will be equivalent to one of those. Each of these points should give rise to six allowed optical transitions, some of which are doubly degenerate in the high-symmetry directions. This large number of allowed modes is not observed in the spectrum. The sharpness of the observed lines suggests that they are not a result of accidental degeneracies of many modes. Moreover, the similarity of the spectra of In_2Te_3, Ga_2S_3, and Ga_2Se_3 suggests that there is a mechanism similar in all these structures that favors certain phonon modes relative to others. Trying to relate this mechanism to the crystal structure, one should recall the fact that the ordered M_2X_3 compounds have one long-range-order feature that is shared by all of them—the existence of continuous uninterrupted connected tetrahedra along the [110] directions.

The phonon mean free path certainly depends on the ordering of the cations. In the disordered structure we expect a stronger scattering of phonons by the lattice vacancies. In this case, their mean free path is comparable to the interatomic distance. This is evidenced experimentally by comparing the lattice thermal conductivities in ordered and disordered In_2Te_3, which are 2.68×10^3 and 1.66×10^3 cal cm^{-1} sec^{-1} K^{-1}, respectively.[1] The phonons that are less susceptible to scattering by vacancies are most likely those which propagate along the uninterrupted chains of tetrahedra in the [110] directions. We will assume that the lines which we observe correspond to phonons originating from the [110] directions in the large BZ. This assumption implies that the phonons in other directions are scattered much more and therefore do not produce intense lines.

All the discussed structures have a sixfold folded BZ in the [110] direction. The reciprocal-lattice points $(2\pi/3a)(1,1,0)$, $(2\pi/3a)$ $(2,2,0)$, and $(2\pi/a)$ $(1,1,0)$ in the large BZ transform into $k=0$ in the real BZ. Therefore the spectra of all the three crystals are expected to be similar as is really the case. For the sake of simplicity, from now on we shall refer to the vibrational modes of the M_2X_3 compounds as optic and acoustic with respect to their character in the large BZ. The terms longitudinal and transverse modes will also be used accordingly although the real modes might be a mixture of both. Directions will also be referred to only with respect to the cubic cell.

Our most comprehensive data were obtained for ordered Ga_2Se_3. Therefore we shall discuss this material in some detail. As is seen in Fig. 1 the intensities of the high-frequency infrared lines which we attributed to the optical branches are much stronger than those of the lower-frequency modes. The Raman spectrum, on the other hand, reveals very sharp and well-defined lines for the acoustic branches while the optic ones are weak and much broader. This supports the idea that the origin of these two groups of lines is different.

In the real BZ an energy discontinuity is expected which will split the bands at the zone boundaries. The large-zone concept will be useful when these discontinuities are small. Several unresolved lines in the infrared spectrum (e.g., those at 60, 71, 84, and 196 cm^{-1}) appear as very closely spaced doublets in the Raman spectrum of Ga_2Se_3 and justify the approach based on folding. The splitting of the modes, however, should not be seen for the folded points which lie on the surface of the large BZ. Therefore, we assigned the relatively intense sharp unsplit lines at 105 and 155 cm^{-1} to the X point of the large BZ as TA and LA modes, respectively. An additional support of our model is the appearance of extra lines in the infrared spectra of Ga_2S_3 (at 148 and 353 cm^{-1}) and Ga_2Se_3 (at 105 and 244 cm^{-1}) compared to the In_2Te_3 spectrum. These lines were assigned as zone-boundary modes in the large BZ. Selection rules for the transverse modes at the zone boundary allow them to be infrared active when folded to $k=0$ but it was shown by Montgomery[26] that their dipole moment vanishes. This will be true for the cubic structure of In_2Te_3; however, the distortion of the cubic lattice in Ga_2S_3 and Ga_2Se_3 will result in a finite dipole moment and infrared activity for these modes.

For the calculations of the phonon dispersion curves in the ZB structure we used the rigid-ion model.[27,28] This model takes into account short-range central and noncentral forces for nearest neighbors and central forces between second nearest neighbors. In addition, it contains the long-

TABLE I. Values of the rigid-ion-model parameters for the M_2X_3 compounds. a is the lattice constant; an average value was taken for the distorted structures of Ga_2Se_3 and Ga_2S_3. See text for explanation of the two sets of fitting parameters for In_2Te_3.

		Ga_2Se_3	Ga_2S_3	In_2Te_3 (a)	In_2Te_3 (b)
α	(dyn/cm)	34760	39060	25380	24760
β	(dyn/cm)	40440	46350	46060	40640
μ_1	(dyn/cm)	10600	7768	5118	5899
μ_2	(dyn/cm)	−3450	2545	−4636	−4973
z		1.11	1.06	1.36	1.21
a	(Å)	5.46	5.24	6.165	6.165

range Coulomb interactions. The symmetry of the lattice requires a force-constant matrix for the nearest neighbors of the form

$$\begin{bmatrix} \alpha & \beta & \beta \\ \beta & \alpha & \beta \\ \beta & \beta & \alpha \end{bmatrix},$$

and for the second nearest neighbors,

$$\begin{bmatrix} \mu_i & \nu_i & \delta_i \\ \nu_i & \mu_i & \delta_i \\ -\delta_i & -\delta_i & \lambda_i \end{bmatrix}, \quad i=1,\ 2.$$

Following Smith[29] we assume $\delta_i=\lambda_i=0$ and $\mu_i=\nu_i$. The total effective ionic charge is ze. In this form it is a five-parameter model with α, β, μ_1, μ_2, and z as the adjustable parameters. The rigid-ion model is chosen because of its simplicity and the fact that despite its deficiencies, it has predicted reasonable dispersion curves for all the cases of the ZB-structure materials.[30,31] The main discrepancies between the observed and calculated dispersion curves are found for the TA modes. This, in turn, makes the calculation of the elastic constants unrealistic if the model parameters are determined from the phonon spectra. The reasons for this are discussed by Keating.[32] We shall not elaborate further on this point as our purpose is only to show a general trend in the model parameters that can be fitted into the already known trends in the simple ZB-structure materials.[31]

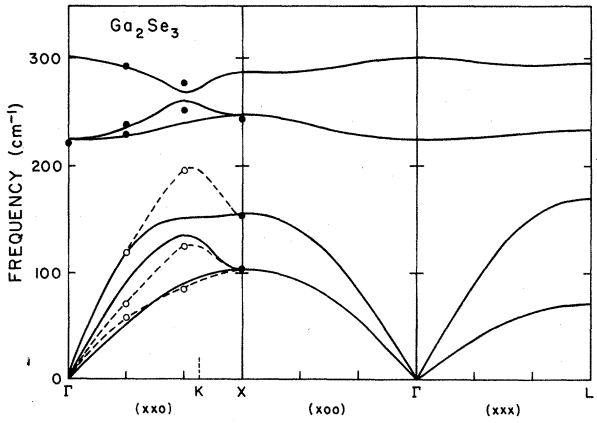

FIG. 8. Dispersion curves for Ga_2Se_3 in the large BZ as calculated using the parameters of Table I. The data points which were used for the fit are indicated by full circles, all the others by open circles. The dashed lines indicate the dispersion obtained by interpolation of the experimental data. The k vector is measured in units of $2\pi/a$ (the plotted $x=ka/2\pi$).

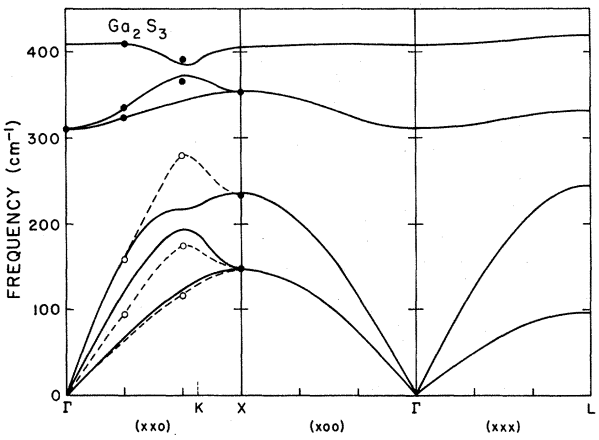

FIG. 9. Dispersion curves for Ga_2S_3 (same notations as in Fig. 8).

A nonlinear least-squares fit program was used for obtaining the five adjustable parameters which are given in Table I for the three crystals. The calculated dispersions in the large BZ for the Σ, Δ, and Λ directions are given in Figs. 8, 9, and 10, which include also the experimental points assigned to the dispersion curves in the [110] direction. The ordering of the experimental points along the dispersion curves in the large BZ is somewhat arbitrary. Thus, for example, each of the ZB optical branches can be curved upwards or downwards. This gives at least four different arrangements of the experimental points which give four different sets of parameters. In practice, however, very little freedom is allowed in the calculations, and any arrangements other than those shown in the figures gave much inferior fits. Only minor changes could be made in the identifications of the modes deduced from the optical branches without drastically changing the accuracy of the fit. Some ambiguities exist for the modes deduced from the acoustic branches; however, different assignments affect the parameters only slightly. In our final analysis we included only the zone-

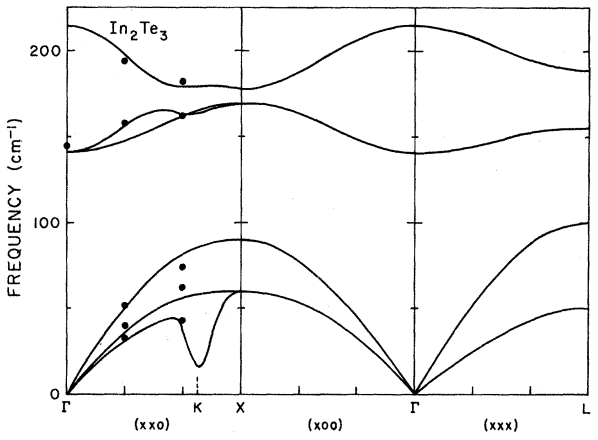

FIG. 10. Dispersion curves for In_2Te_3 calculated by set (a) of parameters of Table I (same notations as in Fig. 8).

edge frequencies of the acoustic branches in the fit for Ga_2Se_3 and Ga_2S_3. The values of these frequencies for Ga_2S_3 were chosen by scaling the corresponding values of Ga_2Se_3 and using the spectral lines of Ga_2S_3 that were close to the calculated frequencies. The points that were used for the fit are indicated by full circles in Figs. 8 and 9. The obtained fit describes fairly well the frequencies of the observed phonon modes in these crystals including the points that were not used in the fitting process (open circles in the figures). A large discrepancy occurs for one point—the LA mode at $(\frac{2}{3}, \frac{2}{3}, 0)$.

The situation is less clear for In_2Te_3, where the measured data give less information about the vibrational modes. Two ways were tried for fitting the data. The first is described by set (a) of the parameters in Table I; its dispersion curves are plotted in Fig. 10. This was done by fitting all the points to the model, as can be seen in the figure. Set (b) of Table I was obtained by including only those acoustic frequencies which were assigned to the LA mode. It can be seen that the parameter α is almost unchanged while all the others are changed by about 15%. We do not consider our model precise enough to account for such changes. The parameters that we obtained are therefore assumed to be related, at least in a qualitative way, to the real force constants in the crystals.

The central and noncentral nearest-neighbor force constants are compared with those of nondefect ZB materials[31] in Figs. 11(a) and 11(b). It is noted by Kunc[31] that these force constants vary monotonically with the interatomic distances within each group (II-VI, III-V, etc.). This is stated in Ref. 31 only for the parameters of the deformation dipole model, but it is apparent from the figures that the same is true for the rigid-ion model. The parameters that we obtained follow the same trends. The central-force constants α for the M_2X_3, compounds have intermediate values between those of the II-VI and the III-V compounds, but our noncentral-force constants have higher values than those for the other two groups. The values of this parameter for In_2Te_3 are higher than those for Ga_2Se_3 and Ga_2S_3.

The magnitude of the phonon frequencies in the rigid-ion model is determined mostly by the nearest-neighbor central-force constant α. The noncentral-force constant β influences the curvatures within each band. Changes in β affect mostly the TA branches to which the elastic constants are sensitive. The intermediate values we found for

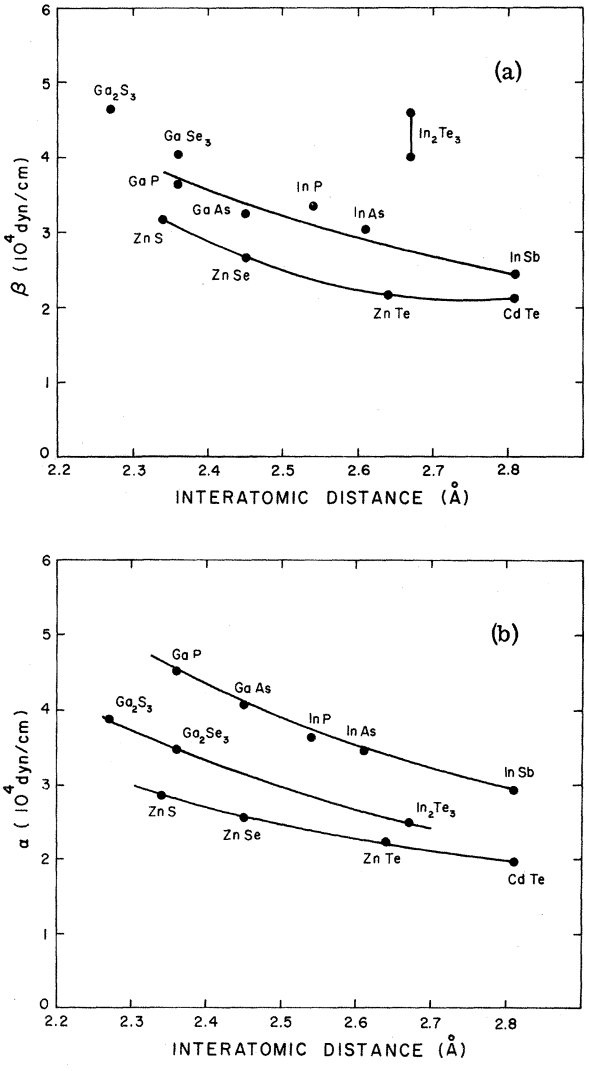

Fig. 11. Central (a) and noncentral (b) nearest-neighbor force-constant parameters for the rigid-ion model plotted versus the interatomic distances in II-VI, III-V, and M_2X_3 compounds.

α are expected with regard to Van Vechten and Thurmond's remark[24] that the changes in frequencies induced by the vacancies are small. The noncentral forces are expected to be changed more significantly by the presence of vacancies.

In this regard we should note that Keating[32] attributes the unrealistic results for the relations between the elasticity and the lattice dynamics in the rigid-ion model to the erroneous use of the noncentral first-neighbor force constant in this mode. The discrepancy could be even higher in our case where the noncentral-force constants should play a more significant role because of the vacancies.

An interesting trend is observed in the lower TA mode of In_2Te_3. This mode approaches a deep minimum at the edge of the large BZ in the Σ direction (which is at $x = 0.75$). We obtained this result whether we included the experimental points of the low TA modes in the fit or not. The fact that this mode almost goes soft might indicate that the balance of the interatomic forces which enables the crystal to maintain its cubic symmetry is very delicate. This result may be fortuitous; however, if it is not an artifact of our model, it would suggest that a structural phase transformation may be observed in In_2Te_3 at low temperature which will result in a more stable structure with distorted tetrahedra as in the other ordered compounds.

VI. CONCLUSIONS

The lattice vibrations of ordered-defect-ZB- and wurzite-structure semiconductors In_2Te_3, Ga_2S_3, and Ga_2Se_3 were studied by far-infrared and Raman scattering techniques. It was found that the spectra were relatively simple despite the large unit cell in these materials. Moreover, all the spectra were similar in spite of different crystal symmetries of the three compounds. We suggested a model which is based on the similarities in all these structures, namely, the presence of uninterrupted chains of tetrahedra along the [110] directions. It relates the observed spectra to the vibrational spectra of the simple ZB structure. The model is based on a sixfold folding of the ZB BZ in the [110] direction. By fitting the observed spectra by a rigid-ion model we obtained the dispersion relations of the corresponding ZB structure. A comparison of the calculated force constants with those of III-V and II-VI compounds shows that the presence of defects affects the central forces between nearest neighbors only slightly while the noncentral forces are changed more significantly.

The success of this approach suggests that in some materials the vibrational modes are not strongly affected by the presence of ordered vacancies. In this case their presence only changes the selection rules. It is well known that vacancies randomly distributed in crystals relax the k-conservation rule and make the whole vibrational spectrums of the unperturbed crystal infrared or Raman active. We have shown that when the vacancies are ordered only certain vibrational modes of the unperturbed crystal become active, and have suggested and tested a method for finding these frequencies.

In the case of In_2Te_3 the calculated dispersion relation shows a tendency of softening of a TA phonon at the zone boundary in the [110] direction. This suggests that the cubic structure of ordered In_2Te_3 may be subject to a phase transition to lower symmetry structures similar to those of Ga_2Se_3 and Ga_2S_3.

ACKNOWLEDGMENTS

The authors would like to thank M. F. Thorpe for his observation on this work, J. F. Vetelino for his rigid-ion model computer program, T. R. Kirst for technical assistance, and G. B. Fisher for his comments on the manuscript.

---

*Work supported by a grant from the National Science Foundation. It has also benefitted from the general support of Materials Science at Brown University by the NSF.

†Present address: Dept. of Electrical Engineering, Technion, Haifa, Israel.

[1]N. A. Goryunova and S. I. Radautsan, *Soviet Research in New Materials*, edited by D. N. Nasledov and N. A. Goryunova (Consultants Bureau, New York, 1965), p. 1.

[2]H. Krebs discusses various examples of these structures in *Fundamentals of Inorganic Crystal Chemistry* (McGraw-Hill, New York, 1968).

[3]H. Hahn and W. Klinger, Z. Anorg. Chem. 259, 135 (1949); 260, 97 (1949); H. Hahn, Angew. Chem. 64, 203 (1952).

[4]H. Inuzuka and S. Sugaike, Proc. Jap. Acad. 30, 383 (1954).

[5]J. C. Wooley, B. R. Pamplin, and P. J. Holmes, J. Less-Common Met. 1, 362 (1959).

[6]A. I. Zaslavskii, N. F. Kartenko, and Z. A. Karachentseva, Fiz. Tverd. Tela 13, 2562 (1971) [Sov. Phys.-Solid State 13, 2152 (1972)].

[7]G. Harbeke and G. Lautz, Z. Naturforsch. A 13, 771. (1958).

[8]A. I. Zaslavskii and V. M. Sergeeva, Fiz. Tverd. Tela 2, 2872 (1960) [Sov. Phys.-Solid State 2, 2556 (1961)].

[9]J. Goodyear and G. A. Steigmann, Acta Cryst. 16, 946 (1963).

[10]L. S. Palatnic and E. K. Belova, Neorg. Mater. 1, 1883 (1965) [Inorg. Mater. 1, 1703 (1965)].

[11]V. P. Zhuze, V. M. Sergeeva, and A. I. Shelykh, Fiz. Tverd. Tela 2, 2858 (1960) [Sov. Phys.-Solid State 2, 2545 (1961)].

[12]G. Harbeke and G. Lautz, Z. Naturforsch. A 11, 1015 (1956).

[13]V. A. Petrusevich and V. M. Sergeeva, Fiz. Tverd.

Tela 2, 2881 (1960) [Sov. Phys.-Solid State 2, 2562 (1961)].
[14]G. Harbeke and G. Lautz, Z. Naturforsch. A 13, 775 (1958).
[15]D. Bidjin, S. Popovic, and B. Celustka, Phys. Status Solidi A 6, 295 (1971).
[16]D. L. Greenaway and M. Cardona, *Proceedings of the International Conference on the Physics of Semiconductors at Exeter* (Inst. Physics, London, 1962), p. 666.
[17]V. V. Sobolev, Phys. Status Solidi B 43, K71 (1971).
[18]A. E. Bakhyshev, L. G. Musaeva, and G. A. Akhundov, Phys. Status Solidi B 54, K77 (1972).
[19]M. I. Karaman, V. P. Mushinskii, and L. I. Palaki, Inorg. Mater. 8, 1301 (1972).
[20]L. G. Musaeva, G. A. Akhundov, A. E. Baknyshev, and N. M. Gasanli, Phys. Status Solidi B 60, K1 (1973).
[21]E. Finkman and J. Tauc, Phys. Rev. Lett. 31, 890 (1973).
[22]A. S. Pine and G. Dresselhaus, Phys. Rev. B 4, 356 (1971).
[23]P. C. Newman, J. Phys. Chem. Solids 23, 19 (1962).
[24]J. A. Van Vechten and C. D. Thurmond, J. Electrochem. Soc. (to be published).
[25]M. F. Thorpe called to our attention a mistake in Ref. 21. If the fcc structure is assumed for the large unit cell the ratio of the lattice constants is 3 instead of 6. In fact, the large unit cell is simple cubic, and the ratio 6 used in Ref. 21 is correct.
[26]H. Montegomery, Proc. R. Soc. A 309, 521 (1969).
[27]L. Merten, Z. Naturforsch. A 13, 662 (1958); 13, 1067 (1958).
[28]R. Banerjee and Y. P. Varshni, Can. J. Phys. 47, 451 (1969).
[29]H. M. J. Smith, Philos. Trans. R. Soc. Lond. A 241, 105 (1948).
[30]J. F. Vetelino and S. S. Mitra, Solid State Commun. 7, 1181 (1969).
[31]K. Kunc, thesis (University of Paris VI) (unpublished); K. Kunc, M. Balkanski, and M. Nusimovici (unpublished).
[32]P. N. Keating, Phys. Rev. 145, 637 (1966).